A Kinesthetic Washout Filter for Force-feedback Rendering

Fabien Danieau, Anatole Lécuyer, Philippe Guillotel, Julien Fleureau, Nicolas Mollet, and Marc Christie.

Abstract—Today haptic feedback can be designed and associated to audiovisual content (haptic-audiovisuals or HAV). Although there are multiple means to create individual haptic effects, the issue of how to properly adapt such effects on force-feedback devices has not been addressed and is mostly a manual endeavor. We propose a new approach for the haptic rendering of HAV, based on a washout filter for force-feedback devices. A body model and an inverse kinematics algorithm simulate the user's kinesthetic perception. Then the haptic rendering is adapted in order to handle transitions between haptic effects and to optimize the amplitude of effects regarding the device capabilities. Results of a user study show that this new haptic rendering can successfully improve the HAV experience.

Index Terms—washout filter, force-feedback, haptic-audiovisuals, user experience, kinesthetic

✦

1 INTRODUCTION

FOR decades research and technology for multimedia entertainment have essentially remained focused on improving image and sound. But this multisensory experience is now extended to others senses, in particular to the sense of touch (haptics). Indeed there is a growing interest among researchers in integrating haptic feedback in audiovisual systems and a new medium emerges from this effort: haptic-audiovisuals (HAV [1]).

Recent works have shown that haptic devices can enhance the audiovisual experience. A user may wear a jacket embedding vibrating motors [2], or hold one [3] or several force-feedback devices [4] while watching a movie. In these works the haptic feedback is designed for the end-device. But thanks to new authoring tools [5], content creators can now add multiple haptic effects to a video, independently from a specific device.

Thus the haptic rendering for HAV needs to adapt these haptic effects to the workspace of the actuator and to handle transitions between the effects. The rendering is straightforward for vibrations motors where stopping an effect means stopping the device. However this leads to problems for force-feedback devices. Since they move in a workspace, they must be stopped in a way that they leave the user in a comfortable position, and that they are able to render a potential future effect. But the position of the device cannot be instantaneously set to the center of the workspace. This would create a "counter-effect" perceived by the user. Existing techniques to optimize the workspace of a force-feedback device are not applicable because it is assumed that the user is active [6]. In our context, the user passively feels the content.

This issue has been solved for motion platforms by a *washout filter* in charge of moving the device to a neutral position in an imperceptible way [7]. For instance, if two "forward accelerations" need to be rendered, the motion platform moves forward, then goes slightly back to its central position, and moves forward again. The intermediary step (i.e. moving to the center) between two effects is not perceived by the user. The platform moves under the perceptual threshold of the vestibular system (around $0.1\ m.s^{-2}$ [8]), assuming that this organ located in the inner ear undergoes the same acceleration as the motion platform. Hence these algorithms are not adapted to force-feedback devices which stimulate the kinesthetic system and so different perceptual thresholds (around 0.5 to $1\ deg.s^{-1}$ depending on the joint [9]). Thus we introduce the use of a washout filter, based on the human kinesthetic perception, for rendering HAV.

2 HAPTIC RENDERING FOR HAV BASED ON A WASHOUT FILTER

We observed in previous work that haptic effects associated to the movement of a camera enhance the HAV experience [4]. The sequences were however limited to one continuous camera movement (one shot). Then if several shots are combined, the actuator would suddenly go back to the central position at the end of an effect, inducing a counter-effect. For example, Figure 1 depicts three separate haptic effects associated to the movements of the camera of a video sequence. Counter-effects occur between each haptic effect (at the end of a shot).

To tackle this issue, we propose a new workflow for the haptic rendering of HAV, based on a washout filter (see Figure 2). Two steps compose the washout filter. First, the perceptual optimizer relies on kinesthetic perceptual thresholds to make the counter-effects imperceptible. Then the workspace optimizer ensures that the maximum space of the workspace is exploited and

- *F. Danieau is with Technicolor R&I, France and Hybrid, Inria, France. e-mail: fabien.danieau@technicolor.com*
- *A. Lécuyer is with Hybrid, Inria, France.*
- *P. Guillotel, J. Fleureau and N. Mollet are with Technicolor R&I, France.*
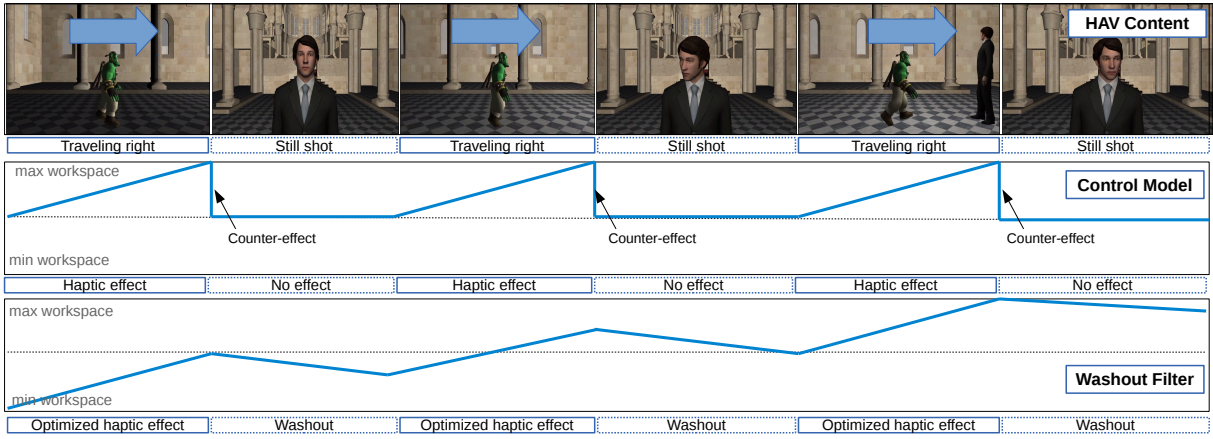- *M. Christie is with MimeTIC, IRISA, France.*

Fig. 1: Schematic example of the use of our approach based on a washout filter. Three effects have been associated to a video. A direct mapping of haptic effects to the workspace of the actuator would generate counter-effects (Control Model). Our washout filter removes them (Perceptual Optimizer) and optimizes the use of the workspace (Workspace Optimizer).

that its limits are respected. This washout filter reduces the counter-effects while preserving the actual effects. Figure 1 shows the results of the washout filter for the three effects of our example.

2.1 Haptic device

This washout filter may be used with any setup composed of several force-feedback devices. As a proof-of-concept, we use here the *HapSeat* [4], a motion simulator based on three force-feedback devices (see Figure 3). The following notation is used in the remainder of this paper. The actuators near to the head, left hand and right hand are labeled H, LA, and RA. Their central positions in their workspaces are named respectively G_H, G_{LA} and G_{RA}, G being the center of the space. The workspace of one actuator is defined by W (in our case Novint Falcons are used. The dimension of W is $10 \times 10 \times 10 \ cm$).

2.2 Haptic effects

A haptic effect E_i of a global set of N haptic effects $E = \{E_i\}_{1 \le i \le N}$ starts at an instant T_i of the video, has a duration of D_i, and is described by M_i, a force (Cartesian coordinates x_c, y_c, z_c) and a torque (three Euler angles
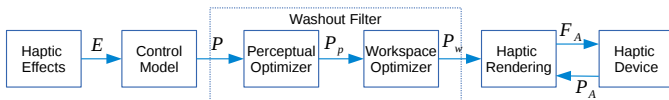

Fig. 2: Workflow of haptic rendering for HAV. Haptic effects E are converted into positions P for the actuator by a control model. The perceptual optimizer removes undesirable effects by limiting the movement of the actuator (P_p), and the workspace optimizer ensures that the limits of the workspace are respected (P_w). The force F_A is then rendered by the device depending on its current position P_A.

ϕ_c, θ_c, ψ_c) at an instant $t \in [T_i, T_i + D_i]$:

$$M_i(t) = [x_c^i(t), y_c^i(t), z_c^i(t), \phi_c^i(t), \theta_c^i(t), \psi_c^i(t)] \quad (1)$$

2.3 Control model

For a given haptic effect E_i, the control model for one local actuator A is formulated in terms of displacement from its initial and central position G_A to the new position G'_A, $\forall t \in [T_i, T_i + D_i]$:

$$\overrightarrow{G_A G'_A}(t) = f(\vec{L}(t), \vec{R}(t)) \quad (2)$$

where

$$f(\vec{L}(t), \vec{R}(t)) = \frac{\|\vec{L}(t)\|\vec{L}(t) + \|\vec{R}(t)\|\vec{R}(t)}{\|\vec{L}(t)\| + \|\vec{R}(t)\|} \quad (3)$$

and

$$\vec{L}(t) = \begin{bmatrix} s_x & 0 & 0 \\ 0 & s_y & 0 \\ 0 & 0 & s_z \end{bmatrix} \begin{bmatrix} x_c^i(t) \\ y_c^i(t) \\ z_c^i(t) \end{bmatrix} \quad (4)$$

$$\vec{R}(t) = (R_x(m_x\phi_c^i(t))R_y(m_y\theta_c^i(t))R_z(m_z\psi_c^i(t)) - I_3)\overrightarrow{GG_A}) \quad (5)$$

The function f is the combination of two vectors $\vec{L}$ and $\vec{R}$ which respectively uses the positions and rotations described by the trajectory M_i. From this equation, the new application points G'_H, G'_{LA} and G'_{RA} are computed from the initial points G_H, G_{LA} and G_{RA}. More detailed on this control model are provided in [4].

Eventually the position P computed by the control model for one actuator A can be defined as:

$$P(t) = \begin{cases} \overrightarrow{G_A G'_A}(t), \forall t \in [T_i, T_i + D_i] \\ 0, \forall t \in]T_i + D_i, T_{i+1}[\end{cases} \quad (6)$$

Between haptic effects ($\forall t \in]T_i + D_i, T_{i+1}[$), the actuator goes to the central position, which may induce counter-effects. Hence we propose the following washout filter to remove them.
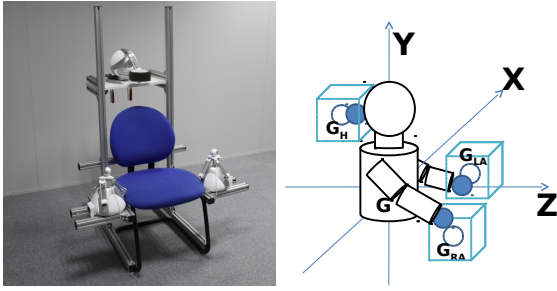
Fig. 3: HapSeat: device (left) and schematic representation of effectors on the user's body (right)

2.4 Washout filter

2.4.1 User's body model

The kinesthetic perception is complex and includes several factors. According to Jones [9], the kinesthetic perception is related to the angular speed of the joints of the moving limb. The faster the movement is, the lower the detection threshold is. Besides the joints do not have the same sensibility: proximal joints are more sensitive than distal ones. Muscles play also a role in the detection threshold which decreases with their contraction.

Our approach consists in designing a user's body model to compute the kinesthetic perception (see Figure 3). In this model we assume that the user is relaxed when watching a video, then the user's perceptual thresholds are determined by angular speeds associated to each joint. The arms are considered as two segments (arm and forearm) and two joints (elbow and shoulder). The head and neck are composed by one segment and one joint respectively. The size of segments and the angle limits of joints are defined by anatomical data [10] and listed in Table 1. Constraints for the shoulders are not necessary due to the small movements of the actuators.

Limb	Size (cm)
Neck and Head	16.8
Forearm	36.2
Arm	34.9
Positions	**x,y,z (cm)**
Left Shoulder	(30,30,0)
Right Shoulder	(-30,30,0)
Base Neck	(0,30,0)
Left Actuator (G_{LA})	(30, -10, 40)
Right Actuator (G_{RA})	(-30, -10, 40)
Head Actuator (G_{HA})	(0, 46.8, 0)
Constraints	**Angle (deg.)**
Elbow	0 to 140
Head (pitch)	-65 to 40
Head (yaw)	-50 to 50
Head (roll)	-35 to 35

TABLE 1: Biomechanical constraints and parameters used in our model.

2.4.2 Perceptual optimizer

The perceptual optimizer consists in moving the actuator toward its central position in a way that this movement is not perceived by the user. Hence the actuator speed needs to stay under the user's perceptual threshold.

Given the skeleton of an arm composed by segments and joints and the given target position of the hand, multiple combinations of angular speeds are possible. This kind of problem, well known in computer animation, is solved by inverse kinematics algorithms. We use here the "cyclic coordinate descent" (CCD) algorithm which is effective for simple configurations with small movements [11].

The new position P_p of the actuator computed by the perceptual optimizer can be defined as:

$$P_p(t) = \begin{cases} P_p(T_i) + P(t), \forall t \in [T_i, T_i + D_i] \\ P_p(t - \Delta t) + v\Delta t, \forall t \in]T_i + D_i, T_{i+1}[\end{cases} \quad (7)$$

with Δt the sampling time (typically $20\ ms$) and

$$v = \underset{0 \leq K(v,t)}{\arg\min}(\|P(t - dt) + v\Delta t\|) \text{ and } P_p(0) = 0 \quad (8)$$

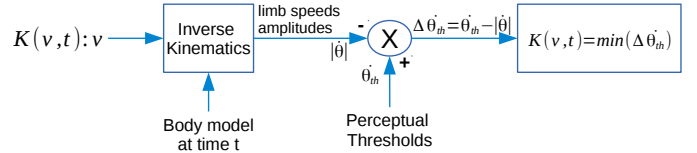and the function K defined in Figure 4.

Fig. 4: Function K computing the speed of the actuator. The angular speeds of the joints are determined from the current speed v of the actuator. The speeds constrained by the perceptual thresholds are then calculated.

The position P_p is thus constrained by the perceptual thresholds when $t \in]T_i + D_i, T_{i+1}[$. P_p can be also written:

$$P_p(t) = [P_p^1(t), P_p^2(t), P_p^3(t)]^T \quad (9)$$

where P_p^1, P_p^2, P_p^3 are the positions of P_p for the axes X, Y and Z respectively.

2.4.3 Workspace optimizer

The previous step does not guarantee that the positions computed respect the limits of the workspace W. The workspace optimizer makes sure that these positions remain in the workspace. An offset is performed to use the maximum space (O_p), and if necessary, the amplitude of the haptic effects is reduced (s^*). The new position computed by the workspace optimizer can be formalized as:

$$P_w(t) = \begin{cases} P_p(t) \text{ if } \forall t, P_p(t) \in W \\ \dfrac{P_p(t) - O_p}{s^*} \text{ else} \end{cases} \quad (10)$$

with

$$s^* = \min(s | \forall t, \frac{P_p(t) - O_p}{s} \in W) \quad (11)$$

where $s \geq 1$ and

$$O_p = [O_p^1, O_p^2, O_p^3]^T \quad (12)$$

where

$$O_p^i = \left\{ \frac{\max_t(P_p^i(t)) - \min_t(P_p^i(t))}{2} \right\}_{1 \leq i \leq 3} \quad (13)$$

2.5 Haptic rendering

The washout filter provides, at each instant t, the target position P_w for each actuator A. The actual force $\vec{F_A}$ applied to an actuator A is computed from a spring-damper model:

$$\vec{F_A} = k(\vec{P_w} - \vec{P_A}) - d\vec{V_A} \qquad (14)$$

where $\vec{P_w}$ is the targeted position, $\vec{P_A}$ the current position of the actuator, $\vec{V_A}$ its velocity, k the spring constant and d the damping constant.

2.6 Implementation

2.6.1 Perceptual thresholds

The perceptual thresholds are key values in our system because they determine how much the counter-effects can be reduced. Three profiles corresponding to three perceptual thresholds have been designed (see Table 2). First one, entitled T1, is based on Jones' results [9]. The perceptual threshold for the elbow is around $1\ deg.s^{-1}$ (angular speed of the joint). Proximal joints are known to be more sensitive than distal joints, thus we propose to set the thresholds for the shoulder and the neck to $0.5\ deg.s^{-1}$. Such angular speeds are small which constrains the actuators to move very slowly. The positions P_p computed might probably not fit the workspace, so the scaling factor s^* applied by the workspace optimizer could strongly reduce the actual effects. Thus we also propose profiles T2 and T3 with less restrictive constraints to preserve the amplitude of the effects. The underlying hypothesis is that in a context of HAV, the user's attention is split between haptic and audiovisual feedback. Movements of an actuator might not be perceived with higher thresholds. As the output of the washout is non linear, determining such thresholds is not trivial. They were set empirically.

Joints	T1	T2	T3
Neck	0.5	1.5	3
Shoulder	0.5	1.5	3
Elbow	1	2.5	4

TABLE 2: Different values of perceptual thresholds corresponding to the three proposed profiles ($deg.s^{-1}$).

2.6.2 Performance evaluation

We have first measured the time required for each profile to move an actuator from the limit of its workspace to the central position ($5\ cm$ in our case). As expected, the lowest the perceptual threshold, the longest the time required to reach the central position: $1.8s$ for T3, 4.7s for T2 and more than $10s$ for T1 (see Figure 5).

Second, we have evaluated the impact of each profile on the amplitude of the filtered effects (see Figure 6). We have created several 15-second sequences with two to seven successive and identical effects (similarly to the example depicted in Figure 1). This is the most critical situation for the haptic rendering: the actuator has to
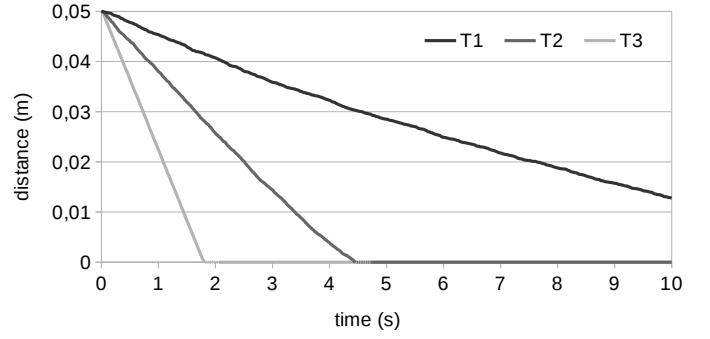

Fig. 5: Time required to move from the edge to the center of the workspace for each profile, T1, T2 and T3.

go several times in the same direction. The more there are effects for a given duration, the less there is time available for the perceptual optimizer. Thus the scaling s^* applied by the workspace optimizer may decrease the amplitude of effects. In our test scenario, starting from two consecutive effects, a scaling factor is applied with profile T1. As expected, the profile T2 less impacts the amplitude and the profile T3 even less. But at some point the scaling is necessary for each profile.
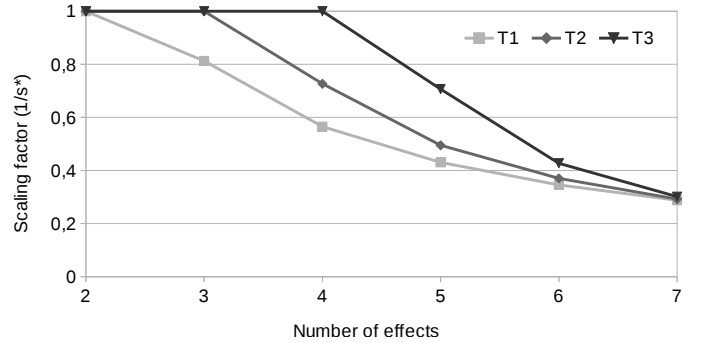

Fig. 6: Scaling factor applied by the workspace optimizer. The more effects there are in a sequence, the more down-scaled they are.

To conclude on this section, we observe that the profile T1 removes the counter-effects, but it has a cost on the amplitude of the actual effects. By increasing the perceptual thresholds, with the profiles T2 and T3, amplitudes are more preserved but the counter-effects may become perceptible.

3 USER STUDY

A user study was conducted to evaluate the influence of our new haptic rendering on HAV experience. Our hypothesis is that the quality of HAV experience is better when counter-effects are not perceived (i.e. in presence of our washout filter). We also wanted to explore the influence of the perceptual thresholds used on this HAV experience.

Twenty participants took part in this experiment, aged from 23 to 52 ($\bar{x}$=39.7 σ_x=9.21). Five were female and three left-handed. None of them was an expert user of force-feedback devices or motion platforms.

3.1 Experimental conditions

We compared four types of haptic feedback: **T1**, **T2** and **T3** respectively computed using the three profiles. The fourth haptic feedback, **T0**, bypasses the washout filter. The haptic rendering is directly computed from the positions P given by the control model. This feedback serves as a control condition to determine how the washout filter and the profiles modify a classical HAV experience.

These four haptic feedbacks were compared against each other for three video sequences of 15 seconds, named **S1**, **S2** and **S3**. They were designed according to the structure depicted in Figure 1: combinations of sequences of a traveling shot of a walking character ($2s$) and a still shot of a man (xs). S1 is composed by a succession of three sequences ($x = 3s$), S2 of four sequences ($x = 1.74s$) and S3 of five sequences ($x = 1s$). A haptic effect was associated to each traveling (movement toward the right). Thus these three sequences exploit the different outputs observed in section 2.6.2.

Hence 4x3 haptic-audiovisual contents had to be experienced by each participant.

3.2 Procedure

The experiment lasted around 20 minutes for each participant, comfortably installed on the *HapSeat*. The study was divided in three steps corresponding to the three sequences S1, S2 and S3. The steps were performed in a random order. For each, the participant had the possibility to experience the video and the four haptic feedbacks. They were asked to try each haptic-audiovisual content, as many times as needed, and to rank the different haptic rendering from 1 (favorite) to 4 (least appreciated). Then they went through the two next steps to experience the two others video sequences and associated haptic feedbacks. This protocol allowed us to order the subjective experiences of the users regarding the different conditions. Finally an informal interview was conducted to collect more information about the user's experience.

3.3 Results

Non-parametric tests were used for the analysis of these ordinal data: Friedman Anova and pairwise Wilcoxon tests with Holm-Bonferroni correction.

The main result of our study is that the three haptic feedbacks provided by the washout filter are preferred to the classical haptic feedback (see Figure 7, F. Anova: $\chi^2 = 96.86, df = 3, p < 0.05$). The three profiles are not statistically different (Wilcoxon test: $p > 0.05$). The statistical analysis of the ranking for each video sequence S1, S2 and S3 provides the same results: the washout filter clearly improves the user's experience, and there is still no significant difference between the profiles. A deeper analysis of the participants' ranking is then necessary.

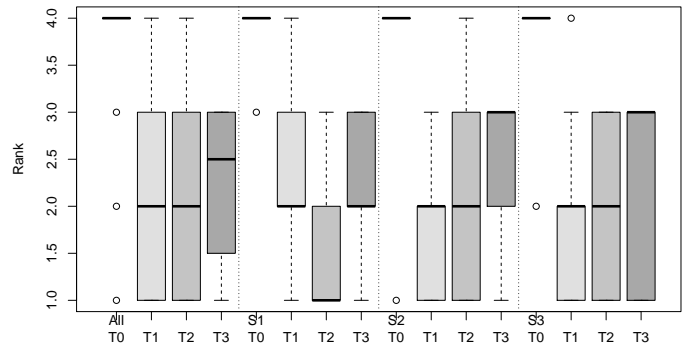We roughly identified three groups of participants during informal post-experiment interviews. Some of

Fig. 7: Rankings for all sequences (the lower the better). Conditions with a washout filter are preferred to the control condition (T0).

them preferred a perfect match between the haptic feedback and the video, when counter-effects were imperceptible. Some preferred more dynamic effects and were more tolerant regarding the perception of counter-effects. So they could better understand when an effect starts and stops. Finally some participants did not have any preference between the three profiles, the results were acceptable in any case. We performed then a hierarchical cluster analysis of the participants' ranking to determine if these three groups could be found [12]. The distance between each participant was computed by a Euclidean distance on the whole set of rankings, and Ward's method was used for the clustering. Results are displayed on a dendrogram where three groups may be identified (cut at height = 8, Figure 8).
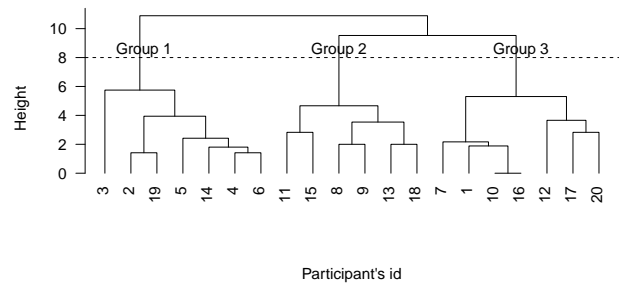

Fig. 8: Dendrogram of the cluster analysis with three identified groups of 6 or 7 participants.

Our observations are confirmed by the analysis of the results of each group. The average ranking for Group 1, from the most preferred to the less, is: T1, T2, T3 and T0 (Figure 9). The four conditions are statistically different (F. Anova: $\chi^2 = 44.71, df = 3, p < 0.05$, Wilcoxon test: $p < 0.05$). Group 3 preferred T2 profile (F. Anova: $\chi^2 = 45.57, df = 3, p < 0.05$, Wilcoxon test: $p < 0.05$), while T1 and T3 are not statistically different. Finally Group 2 reproduces the general result: the three profiles performed better than the T0 but there is no statistical difference between them (F. Anova: $\chi^2 = 33, df = 3, p < 0.05$, Wilcoxon test: $p > 0.05$). Ranking for each sequence was also analyzed but they follow the patterns observed for each group.
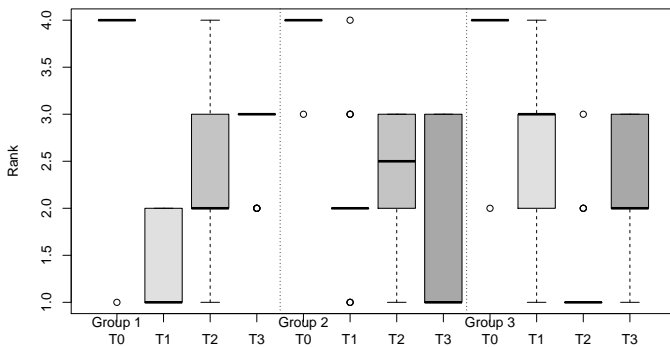
Fig. 9: ranking of the groups for all sequences (the lower the better). Group 1 prefers the profile T1 while Group 3 prefers T2. The three profiles are not statistically different for Group 2.

4 DISCUSSION

Taken together, our results suggest that the use of a washout filter improves the user's quality of the HAV experience. Counter-effects are removed, or at least reduced, which seems to make the haptic-audiovisual content more enjoyable. Nevertheless it appears that the tuning of the washout filter for maximizing the HAV experience depends on the user.

All participants reported that the T1 condition provided continuous movement. This means that the counter-effects were actually not perceived. For Group 1 it seems that the absence of counter-effects is a key component in the quality of experience.

On the contrary Group 2 has found the profile T1 less comfortable than T2. When the effect stopped, these users felt "being frozen" in a position different from the initial position (i.e. when all actuators are at rest). This perception may come from the muscles which do not support the same tension that in the initial position. Our model approximates the kinesthetic perception by the speed of joints and does not include the muscular perception. Then if the speed of the actuator is limited in a way to be not perceived, the off-center position is felt. They also reported that they perceived counter-effects but it was not disturbing due to their weak intensity compared to the actual effects.

From this experiment it seems that some users are mainly disturbed by counter-effects while others are more sensitive to the comfort of the position. But in both cases, counter-effects should be imperceptible. Not necessary from a kinesthetic point-of-view, but rather from a cognitive point-of-view. During a video viewing session, the user's attention is divided between visual, auditory and haptic stimuli. Counter-effects could be not disturbing while above the perceptual thresholds. Hence, in addition to the user's kinesthetic sensibility, the perceptual thresholds for tuning a washout filter might be adjusted depending on the audiovisual context.

5 CONCLUSION

We have presented a new haptic rendering algorithm for force-feedback device in a HAV context. It relies on a washout filter based on the kinesthetic perception. A user's body model is used to compute the angular speed of the joints of the moving limbs. Movement of actuators can be adjusted in order to make undesirable effects imperceptible. The results from our user study show that our novel approach globally improves the HAV experience. Besides, the results provided interesting insights regarding the tuning of such a washout filter. Parameters should be adjusted depending on the user's kinesthetic sensibility and perception of the audiovisual content.

Future work will be dedicated to the potential extension of our approach. In the perceptual optimizer the muscular perception and the user's posture are not considered in the body model. Yet they appear to be important elements to consider in the kinesthetic perception. Concerning the workspace optimizer, it seems that the global scaling may reduce too much the amplitude of the effects. A local scaling would be more adapted.

Others applications are possible for this washout filter, such as adjusting the haptic effects to the user's sensibility or assisting the content creator with an authoring tool (detection of imperceptible or unwanted effects).

REFERENCES

[1] F. Danieau, A. Lécuyer, P. Guillotel, J. Fleureau, N. Mollet, and M. Christie, "Enhancing audiovisual experience with haptic feedback: a survey on HAV," *IEEE Trans. Haptics*, vol. 6, no. 2, pp. 193–205, 2012.

[2] M. Abdur Rahman, A. Alkhaldi, J. Cha, A. El Saddik, and M. A. Rahman, "Adding haptic feature to YouTube," in *ACM Int. Conf. on Multimedia*, pp. 1643–1646, 2010.

[3] D. Gaw, D. Morris, and K. Salisbury, "Haptically annotated movies: reaching out and touching the silver screen," in *Haptic Interfaces for Virtual Environment and Teleoperator Systems*, pp. 287–288, IEEE, 2006.

[4] F. Danieau, J. Fleureau, P. Guillotel, N. Mollet, M. Christie, and A. Lécuyer, "Toward Haptic Cinematography: Enhancing Movie Experienceswith Camera-Based Haptic Effects," *IEEE Multimedia*, vol. 21, no. 2, pp. 11–21, 2014.

[5] F. Danieau, J. Bernon, J. Fleureau, P. Guillotel, N. Mollet, M. Christie, and A. Lécuyer, "H-Studio: An Authoring Tool for Adding Haptic and Motion Effects to Audiovisual Content," in *UIST*, pp. 83–84, 2013.

[6] F. Conti and O. Khatib, "Spanning Large Workspaces Using Small Haptic Devices," in *IEEE World Haptics Conference*, pp. 183–188, 2005.

[7] S.-c. Wang and L.-c. Fu, "Predictive washout filter design for vr-based motion simulator," *IEEE Int. Conf. on Systems, Man and Cybernetics*, vol. 7, pp. 6291–6295, 2004.

[8] L. R. Harris, M. R. Jenkin, D. Zikovitz, F. Redlick, P. Jaekl, U. T. Jasiobedzka, H. L. Jenkin, and R. S. Allison, "Simulating self-motion I: cues for the perception of motion," *Virtual Reality*, vol. 6, no. 2, pp. 75–85, 2002.

[9] L. A. Jones, "Kinesthetic sensing," *Human and Machine Haptics*, 2000.

[10] M. Schuenke, E. Schulte, U. Schumacher, L. M. Ross, E. D. Lamperti, and M. Voll, *General Anatomy and Musculoskeletal System*. Thieme Medical Publishers Inc., 2010.

[11] C. Welman, "Inverse kinematics and geometric constraints for articulated figure manipulation," Master's thesis, Simon Fraser University, 1993.

[12] A. K. Jain, M. N. Murty, and P. J. Flynn, "Data Clustering: A Review," *ACM computing surveys (CSUR)*, vol. 31, no. 3, pp. 264–323, 1999.